



EVOLUTIONARY BIOLOGY

Impact of Holocene environmental change on the evolutionary ecology of an Arctic top predator

Michael V. Westbury^{1*}, Stuart C. Brown^{1,2,3}, Julie Lorenzen¹, Stuart O'Neill², Michael B. Scott⁴, Julia McCuaig⁴, Christina Cheung⁵, Edward Armstrong⁶, Paul J. Valdes⁷, José Alfredo Samaniego Castruita¹, Andrea A. Cabrera¹, Stine Keibel Blom¹, Rune Dietz^{8,9}, Christian Sonne^{8,9}, Marie Louis^{1,10}, Anders Galatius⁹, Damien A. Fordham^{1,2}, Sofia Ribeiro^{11,11}, Paul Szpak⁴, Eline D. Lorenzen^{1*}

The Arctic is among the most climatically sensitive environments on Earth, and the disappearance of multiyear sea ice in the Arctic Ocean is predicted within decades. As apex predators, polar bears are sentinel species for addressing the impact of environmental variability on Arctic marine ecosystems. By integrating genomics, isotopic analysis, morphometrics, and ecological modeling, we investigate how Holocene environmental changes affected polar bears around Greenland. We uncover reductions in effective population size coinciding with increases in annual mean sea surface temperature, reduction in sea ice cover, declines in suitable habitat, and shifts in suitable habitat northward. Furthermore, we show that west and east Greenlandic polar bears are morphologically, and ecologically distinct, putatively driven by regional biotic and genetic differences. Together, we provide insights into the vulnerability of polar bears to environmental change and how the Arctic marine ecosystem plays a vital role in shaping the evolutionary and ecological trajectories of its inhabitants.

INTRODUCTION

The Arctic is among the most climatically sensitive environments on Earth, with increases in temperatures being two- to threefold higher at the northern latitudes than the global mean (1, 2). Within decades, increasing temperatures resulting from Arctic amplification of global warming are expected to lead to the disappearance of multiyear sea ice in the Arctic Ocean (2). These changes in temperature and sea ice cover represent thresholds in Earth's climate system, potentially leading to irreversible ecosystem change (3, 4).

Although the Arctic is currently experiencing marked alterations associated with anthropogenic climate change (5), past environmental and ecological changes linked to climatic shifts in the region are well preserved in paleo-archives (6–8). Paleo-archives reveal, for example, the impact of the Greenland Ice Sheet on the biogeochemistry and productivity of surrounding marine ecosystems (9, 10). These Greenlandic marine ecosystems are further influenced by sea ice cover, sea level fluctuations, changes in ocean circulation, and the availability of nutrients and light for biological

productivity, among others (11). The impact of these changes on the evolutionary ecology of Arctic species is yet to be fully explored.

Changes under environmental conditions can greatly affect the base of the Arctic food web (12). These shifts at the base of the food web drive bottom-up changes in ecosystem structure and function by altering pelagic secondary production, the main food source for all higher trophic-level organisms (13). Shifts in food sources can influence the mobility and connectivity of species (14) and disrupt gene flow among populations, altering evolutionary pathways (15). Nearly all organisms within an ecological community are directly or indirectly tied to the top of the food chain (16). Therefore, an approach to assessing the impacts of environmental change on ecosystems is to investigate apex predators, providing top-down insights into the ecosystem as a whole (17). In the Arctic marine realm, polar bears (*Ursus maritimus*) occupy the top predatory niche. They are found on ice-covered waters across the region and depend on sea ice primarily for hunting pinnipeds (18). Polar bears have been found to inhabit multiyear pack ice in the central Arctic basin, and their preferred habitat is seasonal sea ice, including landfast ice, around the coastline of the Arctic Ocean region (19). This reflects the exploitation of relatively higher levels of biological productivity around seasonal sea ice by seal species (20).

Polar bears have evolved a novel and distinct ecology, behavior, and morphology in response to life in the high Arctic (21). The species is split into 19 management units, determined from a combination of traditional knowledge, radiotelemetry, movements of adult females with satellite radio collars, and genetics (22–24). Greenland is home to at least three management units: Kane Basin and Baffin Bay on the west coast and East Greenland on the east coast (25). A distinct and previously unknown subpopulation was recently documented in the southern coast of east Greenland (26), highlighting that much is still unknown regarding the complexity of polar bear populations around Greenland.

¹Globe Institute, University of Copenhagen, Øster Voldgade 5-7, Copenhagen DK-1350, Denmark. ²Environment Institute and School of Biological Sciences, University of Adelaide, Adelaide, South Australia, Australia. ³Department for Environment and Water, Adelaide, South Australia, Australia. ⁴Department of Anthropology, Trent University, 1600 West Bank Drive, Peterborough, Ontario K9L0G2, Canada. ⁵Department of Anthropology, Chinese University of Hong Kong, Shatin, Hong Kong. ⁶Department of Geosciences and Geography, University of Helsinki, Helsinki, Finland. ⁷School of Geographical Sciences, University of Bristol, Bristol, UK. ⁸Arctic Research Centre (ARC), Department of Ecoscience, Aarhus University, Frederiksborgvej 399, PO Box 358, Roskilde DK-4000, Denmark. ⁹Section for Marine Mammal Research, Department of Ecoscience, Aarhus University, Frederiksborgvej 399, Roskilde DK-4000, Denmark. ¹⁰Greenland Institute of Natural Resources, Kiviq 2, PO Box 570, Nuuk 3900, Denmark. ¹¹Glaciology and Climate Department, Geological Survey of Denmark and Greenland (GEUS), Øster Voldgade 10, Copenhagen DK-1350, Denmark.

*Corresponding author. Email: m.westbury@sund.ku.dk (M.V.W.); elinelorenzen@sund.ku.dk (E.D.L.)

The dependence of polar bears on sea ice makes them a sentinel species for detecting ecosystem tipping points (18). To assess the vulnerability of polar bears to past and future climate and environmental change, it is vital to apply a complementary suite of approaches that combines insights from the present with those of the past (7, 27). Population genomics provide insights into population subdivision and the longer-term demographic history of polar bear populations (21, 28). However, it is difficult to elucidate the drivers underpinning these changes using genetics alone. Dietary tracer analysis of stable carbon ($\delta^{13}\text{C}$) and nitrogen ($\delta^{15}\text{N}$) isotope data and ecological models can provide important additional information for determining biotic and abiotic drivers of past demographic change (29, 30). Stable isotopes can elucidate population-specific foraging behavior and regional primary productivity (31), while ecological models can be used to reveal shifts in the size and area of ecologically suitable habitats in response to climate and environmental changes (7, 30). The incorporation of morphological data can be used to consolidate evolutionary and ecological insights, as changes in morphological phenotype can be shaped by both genetics and the environment (32).

Here, we aim to better characterize the current genomic, morphometric, and dietary relationships among polar bears around Greenland, as well as the role the environment played in shaping their evolutionary ecologies and distributions throughout the Holocene. We focus on integrating independent yet complementary datasets and analyses for polar bears sampled along the coasts of Greenland (Fig. 1A) and make inferences about their evolutionary history and the ecological drivers of similarities and differences between contemporary bears inhabiting the west and east coasts.

RESULTS

Genomics

After mapping to the polar bear reference genome (21), we obtained 106 polar bear nuclear genomes ranging in coverage from $1.7\times$ to $32.8\times$ (including a single $114.1\times$ individual) (table S1). Population structure analyses—principal components analysis (PCA) and admixture proportions—showed clear differentiation between polar bears sampled from the west ($n = 48$) and east ($n = 37$) coasts of Greenland (Fig. 1, B and C, and fig. S1). We did not observe genetic structuring between polar bears sampled from the Kane Basin and Baffin Bay management units of the west coast (fig. S1), in accordance with previous results (22). We found a closer affinity of bears from the west coast to Canadian individuals and of bears from the east coast to the neighboring individuals from Svalbard (fig. S1). The fixation index (F_{ST}) between polar bears sampled from the west and east Greenland coasts was significant (0.0173 ; $P < 2.2 \times 10^{-16}$), further supporting clear genomic differentiation between the two coastlines.

We found that the higher mean observed heterozygosity in west bears (0.000831) compared to east bears (0.000773) (table S2) was significant ($t = 2.6804$, $P = 0.01985$). We did not observe significantly higher mean levels of nucleotide diversity in west Greenlandic bears (0.00033) compared to the east (0.00033) ($t = -0.94269$, $P = 0.3458$). We found three individuals with inbreeding coefficients (probability of two alleles being identical by descent, F) greater than 1%; all three individuals were from the east coast (PB_9, $F = 26.8\%$; PB_28, $F = 3.8\%$; D24082, $F = 2.8\%$).

Estimates of the deeper [>20 thousand years (ka) ago] demographic history of the bears using the pairwise sequential Markovian coalescent (PSMC) model (33) yielded identical demographic trajectories for all individuals analyzed, regardless of their geographic origin or management unit (fig. S2). Results showed relatively stable effective population sizes (N_e) from 150 to ~ 50 ka, after which the joint population experienced a decline in N_e culminating in an approximately 50% decline in N_e by ~ 20 ka. The PSMC results indicated an increase in $N_e \sim 15$ ka, but the reliability of the PSMC model to infer changes in N_e within the past 20,000 years is negligible (33).

Estimates of the more recent (<20 ka) demographic dynamics using stairway plots (34) revealed similar overall demographic trajectories in the west and east groups, with overlapping confidence intervals (CIs) (Fig. 1D). In bears from both coasts, we see a major overall decline in N_e caused by a pattern of several punctuated, rapid declines through time. We investigated the impact of sample size and found the overall trajectories to be similar (fig. S3). The only noticeable difference was an earlier decrease in N_e observed ~ 11 ka in the larger dataset ($n = 12$), which shifted to ~ 13 ka when the number of individuals was downsampled to 9. Hence, the timing of earlier demographic events may be shifted backward in the east Greenland bears ($n = 9$) relative to west Greenland ($n = 12$), due to lower sample size. The trajectories of the stairway plots of the full datasets were similar when specifying the giant panda (*Ailuropoda melanoleuca*), instead of the spectacled bear (*Tremarctos ornatus*), as the ancestral state (fig. S4).

Calculations of genome-wide Tajima's D values uncovered positive values for both west (mean value of 0.196) and east (mean value of 0.030) Greenland bears. A positive score signifies low levels of both low- and high-frequency polymorphisms and may reflect recent population contractions (35). However, only west Greenland bears showed a significant deviation from 0 (west, $P = 0.0003$; east, $P = 0.2837$).

We identified 53 highly differentiated windows (top 1% F_{ST} values) with at least two single-nucleotide polymorphisms (SNPs) among the top 1% of SNPs found to be driving differentiation in the PCA analysis. Eight of these windows contained genes (table S3). Two genes, *SDCCAG8* (36) and *DNASE1L3* (37), have previously been identified as related to body height in human genome-wide association studies, and one, *MAST3* (37), has been associated with body mass.

Stable isotopes

Our $\delta^{13}\text{C}$ (feeding habitat) and $\delta^{15}\text{N}$ (trophic level) data from 31 polar bears comprising 7 bears sampled from the Kane Basin management unit, 6 bears from the Baffin Bay management unit (both west Greenland), and 18 bears sampled from the East Greenland management unit, and their predominant pinniped prey species sampled from the two coasts ($n = 110$; west = 54, east = 56) (table S4) enabled us to assess how the taxonomic composition of diets compared between coasts. After accounting for a decline in $\delta^{13}\text{C}$ values caused by the burning of fossil fuels (the Suess effect), bears from the west coast of Greenland had significantly higher $\delta^{13}\text{C}$ ($U = 14$, $P < 0.001$) and $\delta^{15}\text{N}$ ($t = 8.10$, $P < 0.001$) values, relative to bears sampled from the east coast of Greenland (Fig. 2, A and B). Although west coast bears were sampled from two adjoining management units, we did not observe any significant differentiation in their isotopic compositions ($P > 0.05$) (fig. S5).

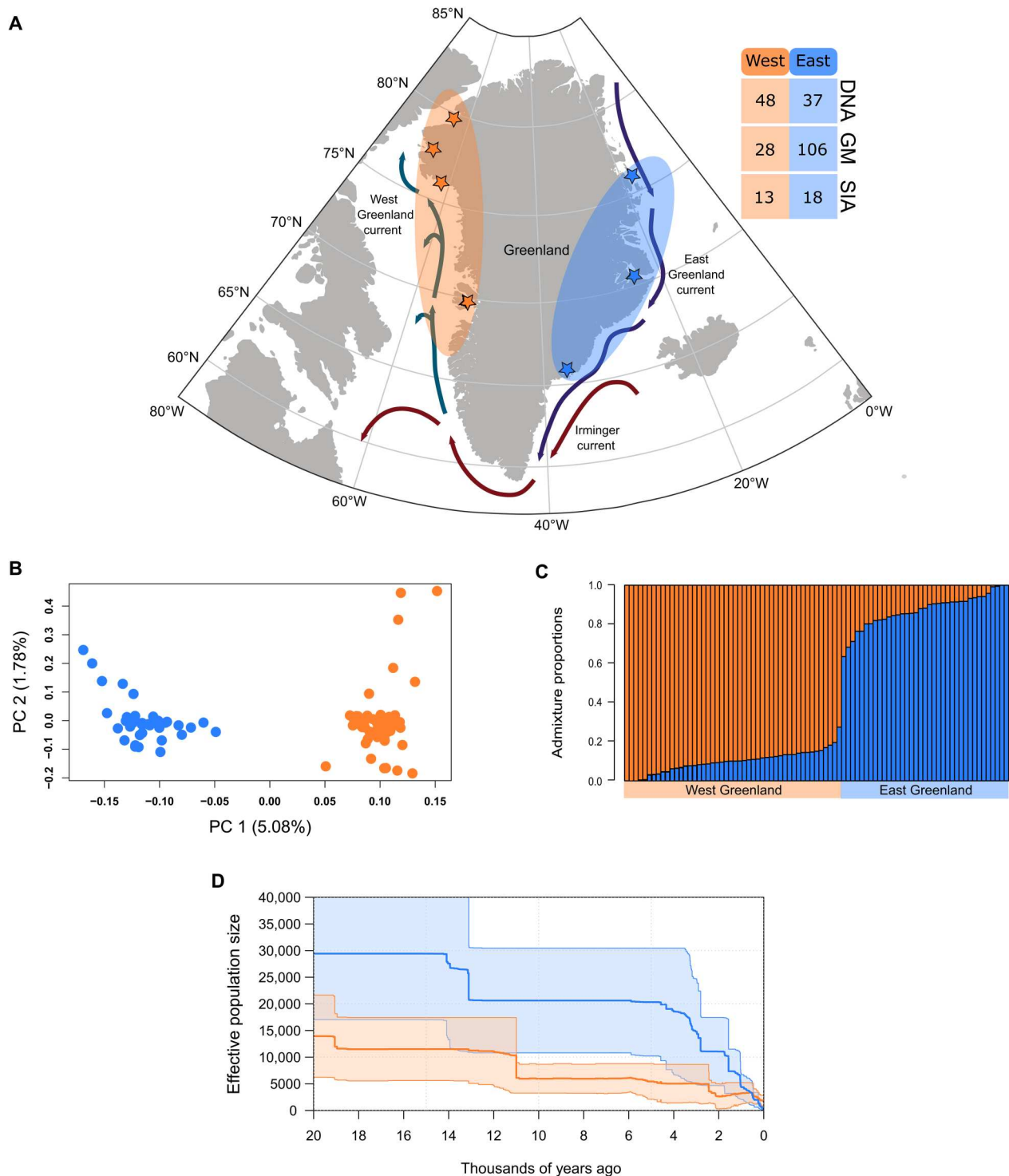


Fig. 1. Sample localities, population structure, and demographic history results. (A) Map of the study area. Shaded areas show the approximate spatial area of sampling locations of the polar bear specimens analyzed from the west (orange) and east (blue) coasts of Greenland. Stars indicate sample sites. Polar bear sample sizes are indicated for genomics (DNA), geometric morphometrics (GM), and stable isotopes (SIA). The study also included genomic data from polar bears sampled in adjoining areas in Canada and Svalbard, and $\delta^{13}\text{C}$ and $\delta^{15}\text{N}$ stable isotope data from the five predominant pinniped prey species of polar bears (bearded seal, harp seal, hooded seal, ringed seal, and walrus); see Materials and Methods for further details. Arrows show ocean currents, modified after (66, 67). (B and C) Genomic population structure analyses based on 85 Greenland polar bears; (B) PCA, with the percentage of variance explained by each component indicated in parentheses; and (C) admixture proportion analysis. (D) Changes in effective population size (N_e) through time inferred using individuals with genome-wide coverages of $>20\times$ (west, $n = 12$; east, $n = 9$) using the site frequency spectrum and stairway plots. Thick lines show the mean N_e values, and shaded areas show 97.5% CIs.

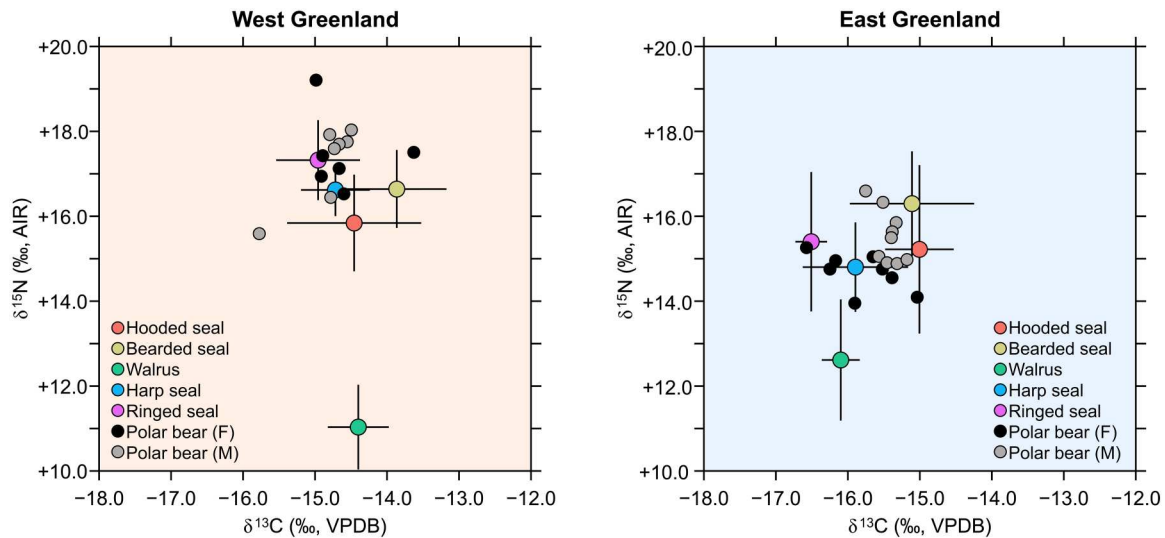


Fig. 2. Comparison of Greenland polar bears and five potential prey bone collagen $\delta^{13}\text{C}$ and $\delta^{15}\text{N}$ values. (Left) West coast and (Right) east coast. Polar bears have been adjusted by -0.5 per mil (‰) for $\delta^{13}\text{C}$ and -4.0 ‰ for $\delta^{15}\text{N}$ to account for the offset between predator and prey. VPDB, Vienna Pee Dee Belemnite reference.

A qualitative comparison of the polar bear and prey isotopic compositions, accounting for trophic discrimination, revealed that bears sampled in west Greenland clustered most closely with ringed seals (*Pusa hispida*), suggesting a diet dominated by this species (Fig. 2A), in agreement with previous work (38). In contrast, bears from the east coast had more varied diets. However, they qualitatively clustered most closely with harp seals (*Pagophilus groenlandicus*) and bearded seals (*Erignathus barbatus*), indicating that their primary prey was harp seal, followed by bearded seal, as well as hooded seal for a few individuals (Fig. 2B).

Within bears from the west, there were no significant sex-based differences in $\delta^{13}\text{C}$ ($U = 20, P = 0.94$) or $\delta^{15}\text{N}$ ($U = 17, P = 0.62$). Although males from the east had higher $\delta^{13}\text{C}$ values than females, this difference was not statistically significant ($t = 2.06, P = 0.07$). Males from the east had significantly higher $\delta^{15}\text{N}$ ($U = 11.5, P = 0.01$) values relative to females from the same area. The higher $\delta^{13}\text{C}$ and significantly higher $\delta^{15}\text{N}$ values in the male relative to female polar bears in the east (Fig. 2B) suggest that females consumed primarily ringed seals and harp seals, while males consumed larger amounts of bearded seals and hooded seals (*Cystophora cristata*). A similar pattern was not observed in polar bears in the west.

Geometric morphometrics

Investigations into shape differences revealed highly significant shape differences ($P < 0.0001$) between polar bear individuals sampled in the west (from both Kane Basin and Baffin Bay management units) and east (from the East Greenland management unit). Despite being from different management units, bears sampled on the west coast did not show significant differences and so were pooled together.

Relative to skulls sampled in the east, skulls from bears sampled in west Greenland were slightly narrower posteriorly and had a temporal fossa that was extended dorsoposteriorly, but anteriorly truncated, an orbit that was slightly compressed dorsally, while the anterior point of the premaxilla was slightly elevated (Fig. 3, A and B). Moreover, 82.1% of the skulls could be correctly reclassified to sampling coast (west versus east) by shape after cross-validation (Table 1). Skulls tended to be largest (centroid) for both sexes in the individuals from the west. However, this difference was only statistically significant for females ($P = 0.006$) but not for males ($P = 0.077$) (Fig. 3C).

Habitat suitability

Ecological niche modeling (ENM) tuning and cross-validation resulted in the optimized model having high geographic transferability shown by low differences between spatial cross-validation folds according to the area under the receiver operating curve values ($\text{AUC}_{\text{diff}} = 0.05$), low 10th percentile training omission rates ($\text{OR}_{10} = 0.13$), and moderate AUC values (0.75 ± 0.05). The model had a greater regularization multiplier (i.e., complexity penalization; $\text{RM} = 3$) and fewer feature classes ($\text{FC} = 3$) than the MaxEnt default ($\text{RM} = 1$ and $\text{FC} = 4$). The ENM had good ability to discriminate between areas of high suitability at known occurrences and background sites for the contemporary period that the model was built on (Boyce index = 0.82; fig. S6).

Our ENM revealed increasing probability of occurrence [hereafter habitat suitability (39)] of polar bears at sea surface temperatures (SSTs) between 0° and $\lesssim 4.5^\circ\text{C}$ (fig. S7), declining to 0 suitability by

Table 1. Success rate of reclassification of specimens to geographical area by skull shape using jackknife cross-validation.

		Allocated to			% Correct
		West coast	East coast	Total	
Origin	West coast	24	4	106	85.7
	East coast	20	86	28	81.1
All skulls		28	106	134	82.1

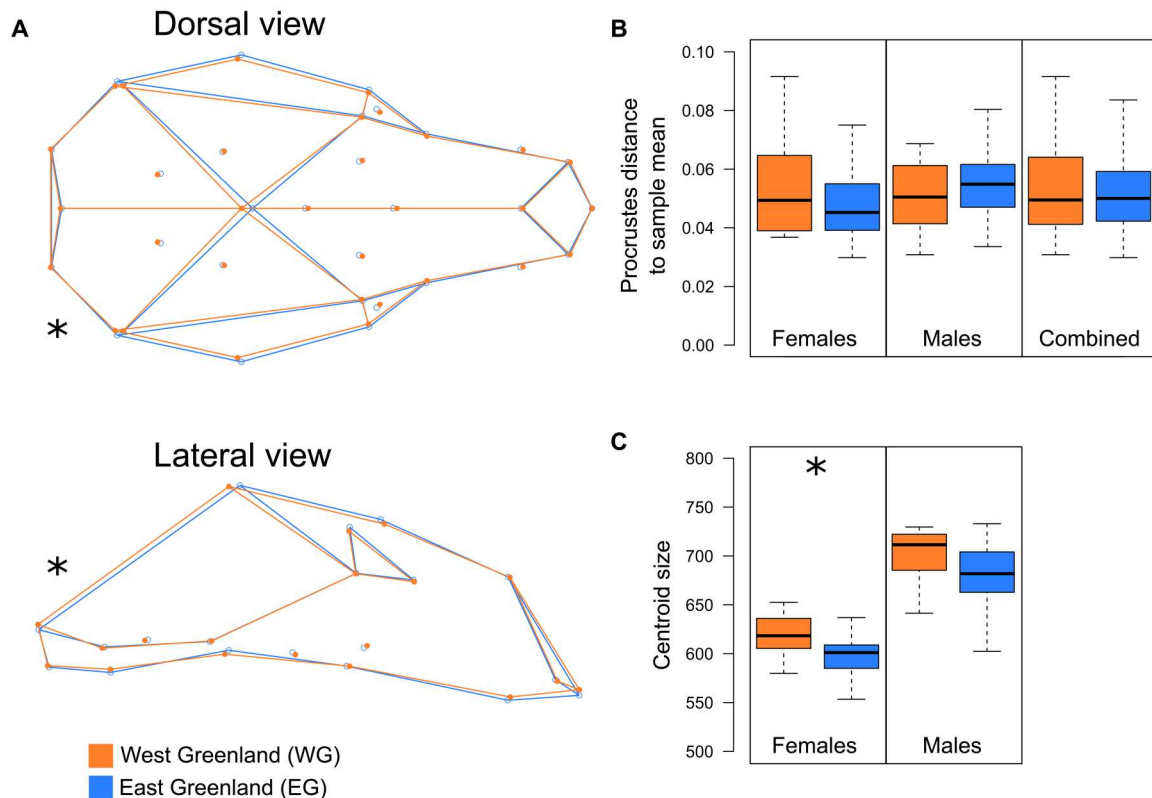


Fig. 3. Geometric morphometric comparisons of 134 polar bears. Samples are pooled into the west (orange, $n = 28$; 14♀, 14♂) and east (blue, $n = 106$; 58♀, 48♂) of Greenland. **(A)** Mean area-specific shapes of polar bear skulls in dorsal and lateral aspects. Correction for allometric effects was performed (see Materials and Methods for further details). Significance of differences ascertained by jackknife cross-validation ($P < 0.0001$). **(B)** Procrustes distances of specimens to the mean of the relevant sample of the whole dataset combined and separated by sex. **(C)** Centroid sizes (square root of sum of squared distances of landmark positions to configuration centroid) of skulls from male and female polar bears from the west and east coasts of Greenland. Differences were statistically significant for females ($P = 0.006$) but not for males ($P = 0.077$). Significance of differences in **(B)** and **(C)** were determined using Student's t tests. Asterisks in **(A)** indicate significant overall shape differences between west and east Greenland bears, whereas in **(C)** indicate significant differences in centroid size in females.

an SST of 15°C. Habitat suitability was positively correlated with annual average sea ice cover and decreased slightly with increasing sea surface salinity. Habitat suitability was not affected by changes in annual variation in fractional sea ice cover or annual variation in SST (fig. S7).

Habitat suitability was high at the beginning of the Holocene (~11 ka) when areal average SST was around 1.5°C, declining sharply with warmer SST values and lower annual average sea ice cover (Fig. 4, A and B, and figs. S8 and S9). The ENM projected a decreasing trend in average habitat suitability from 11 to 4.5 ka, whereafter mean habitat suitability values fluctuated around a long-term stable average (Fig. 4C). Analysis of the center of gravity of habitat suitability indicated a northward shift in the highest habitat suitability values, which correspond to declines in areal habitat suitability (Fig. 4D). All predictor variables show similar patterns to habitat suitability with the exception of SST seasonality, which decreased steadily from a peak of ~7.5 ka (fig. S9). Animations of habitat suitability through time for the study region are provided as a supplementary video (movie S1).

DISCUSSION

Using an integrative, multiproxy approach, we reveal similar evolutionary trajectories, but distinct ecologies, of polar bears sampled from the west and east coasts of Greenland. In doing so, we form hypotheses about the abiotic and biotic factors that have differentially affected the connectivity, demographic history, diet, and morphology of polar bears around Greenland.

Our genomic demographic reconstruction of the past 20,000 years shows a clear pattern of several punctuated, rapid declines in polar bear effective population size (N_e) (Fig. 1D). Although our paleoclimate data and habitat suitability reconstruction extend across the Holocene only, the initial rapid decline in N_e observed in west Greenland bears of ~19 ka may signal the end of the Last Glacial Maximum in the region, a period of massive sea ice loss and increasing temperatures (40, 41). An association between N_e and changes in environment is further evidenced when comparing our genomic demographic reconstructions with paleoclimate and suitable habitat over the past 11,000 years (Fig. 4). Overall, we observe a clear pattern of N_e decline when suitable habitat decreased, which was associated with periods of warmer SST and reduced sea ice cover. SST and sea ice cover are highly correlated, with the latter more likely to be the causative factor driving declines in polar bears, which rely on sea ice for movement, mating, and

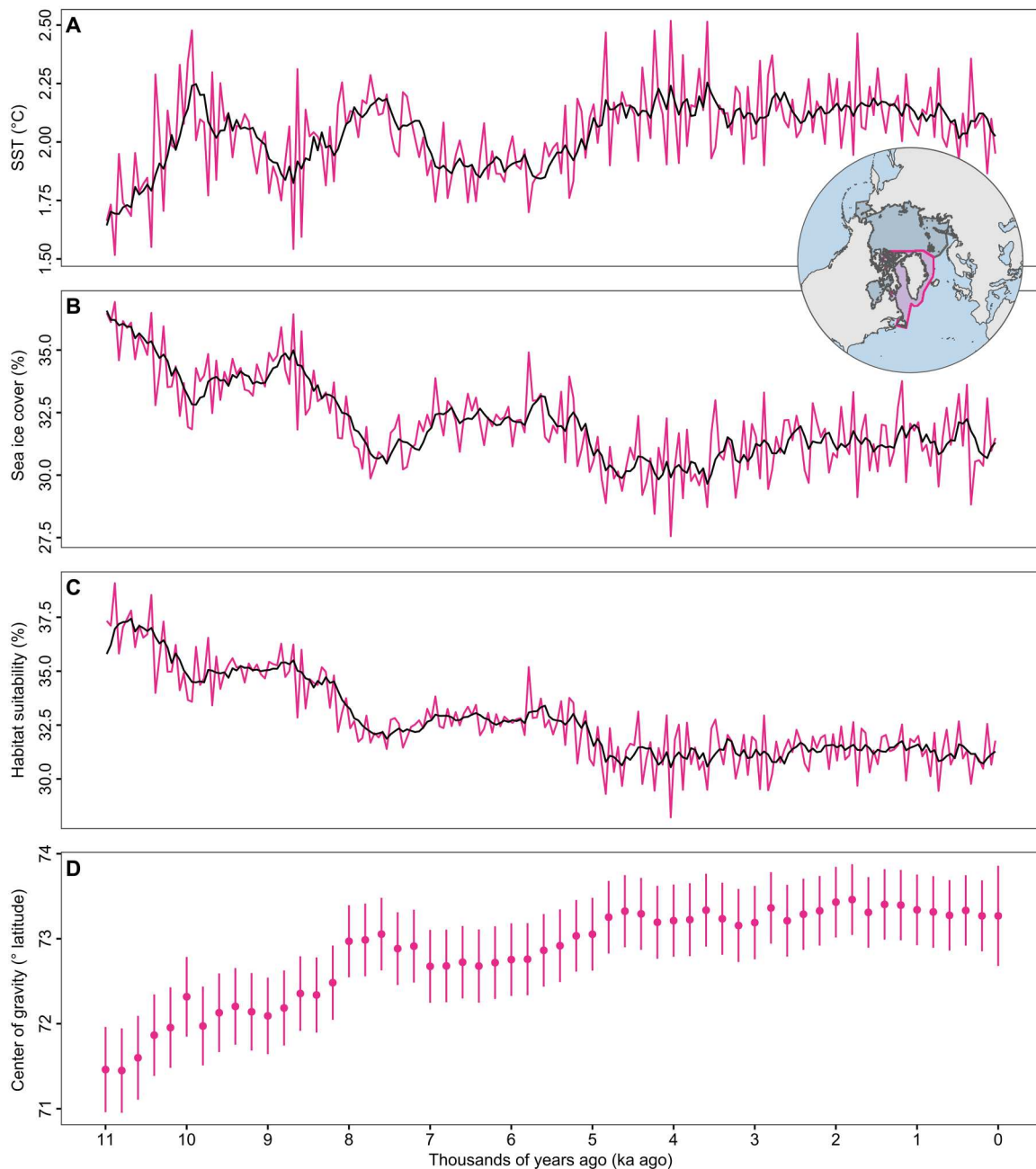


Fig. 4. Areal means of the variables used in the ecological niche modeling and predicted habitat suitability from 11 to 0 ka. The panels show the areal mean values in (A) sea surface temperature (SST), (B) percentage sea ice cover, (C) mean habitat suitability, and (D) average latitude of suitable habitat for the Greenland study region. Pink lines in each plot show 1000-year smoothed mean values. The inset map shows the circumpolar distribution of polar bears in gray and the Greenland subregion in pink.

hunting (42). There is evidence from contemporary populations of declines in polar bear survival and body condition associated with sea ice loss (43–45), and increased overall vulnerability of modern populations has been predicted as sea ice continues to decrease in the near future (46).

Although associated with large CIs, the major and rapid decline in N_e in west Greenland bears observed at the onset of the Holocene of ~11 ka (Fig. 1D) coincided with a simultaneous (i) decline in Greenland-wide mean suitable habitat of ~1.5% (range =

–41:21% change in habitat suitability across the entire study area); (ii) increase in range-wide mean SST of ~0.5°C (range = –0.2:1.2°C); and (iii) reduction in range-wide mean annual sea ice cover of ~4% (range = –25:0% sea ice cover) (Fig. 4, A to C). We also observed a coincident shift in the center of gravity of habitat suitability to higher latitudes (Fig. 4D), suggesting that the decrease in suitable habitat caused a northward shift of the bears, potentially driven by decreasing annual sea ice cover in the southern range. We observe a decline in mean N_e in the east Greenland bears

at a slightly older time period of ~13 ka (Fig. 1D). The discordance between the demography of the east Greenland bears and climate could reflect a smaller dataset (12 bears in west versus 9 bears in east); we show that estimates of population fluctuations may become artificially older when fewer individuals are included in the analysis (fig. S3).

We also observe a rapid decline in N_e in polar bears from east Greenland at approximately 4.5 ka (Fig. 1D). This broadly coincides with the end of the Holocene Thermal Maximum (~5 ka) (47), a decline in habitat suitability of ~1.3% (range = -50:22%), an increase in range-wide mean SST of ~0.2°C (range = -0.5:1.4°C), and a reduction in annual range-wide average sea ice cover of ~3% (range = -34:3%) (Fig. 4). These align with a shift in the center of gravity of habitat suitability to higher latitudes, again suggesting that the decreases in suitable habitat may be caused by a loss of suitable habitat in the south of the range.

A decline in N_e may reflect either decreasing census population size or loss of population connectivity. The latter was not supported by our habitat models. We did not observe any increase in fragmentation of suitable habitat at 11 ka or during the Holocene Thermal Maximum (movie S1) and therefore propose that the observed declines were driven by a decrease in census population size.

We observed additional recent rapid declines in N_e over the past 3000 years, with a sharp decrease in east Greenland ~3 ka and in west Greenland ~2 ka and additional decreases on both coasts from ~1 ka. However, we did not observe any notable concurrent changes in suitable habitat nor in the individual paleoclimate proxies used in our analysis (including SST, sea ice cover, and salinity) (Fig. 4, A and B, and fig. S8). This may reflect the temporal resolution of our climate data (48), which is based on long-term climatic means that have been shown to affect ecological responses to environmental and climatic variables (49). It is noticeable that the recent population declines beginning ~1 ka coincide with the medieval climate anomaly, a period in which marine and lake multiproxy records suggest that the North Atlantic was atypically warm (6). Similar to our findings at the end of the Holocene and during the Holocene Thermal Maximum, this further supports that increased temperatures and concurrent declines in sea ice cover may have detrimental effects on polar bear population size and/or connectivity.

The long-term association between declines in N_e and corresponding increases in SST and decreases in sea ice cover across the past 11,000 years suggests that ongoing global warming may consequently have major detrimental effects on polar bear populations around Greenland. Simulated ocean warming patterns under a range of different future climate scenarios [Shared Socioeconomic Pathways (SSP)] show extensive SST warming around Greenland (90% CI SSP1 to SSP2.6 = -0.8 | 2.4°C; 90% CI SSP5 to SSP8.5 = 0.6 | 5.4°C, above 1981 to 2010 baseline) and reductions in annual sea ice extent by the end of the century (90% CI SSP1 to SSP2.6 = -17.3 | -1.9%; 90% CI SSP5 to SSP8.5 = -32.8 | -13.7%, from 1981 to 2010 baseline), even under reduced emission scenarios (50). It is expected that the Arctic will become essentially ice-free in summer before the end of the 21st century but is very likely to remain sea ice covered during winter for all warming scenarios (51).

We observed notably similar patterns of demographic change throughout the past 150,000 years in our PSMC results, suggesting that bears from the two coasts either responded in identical manners to past environmental changes or that they comprised a

single evolutionary unit and were likely panmictic until the very recent past (fig. S2). The latter is congruent with our analyses of population subdivision that showed significant, albeit low ($F_{ST} = 0.0173$), levels of genomic differentiation between bears sampled from west and east Greenland, with some degree of admixture (Fig. 1C). Differentiation between coasts was further documented by our dietary and morphological analyses of the bears, which indicated distinct foraging ecologies, with significant differences in skull shape and size based on locality (Figs. 2 and 3). Our findings across datasets (genetics, stable isotopes, and morphometrics) indicate clear differentiation and a putative ecologically driven genetic division rather than through longer-term evolutionary forces.

Further supporting a recent divergence is our finding of consistent and continuous suitable habitat over the north of Greenland throughout the Holocene (movie S1), which is likely to have facilitated movement and connectivity between west and east. The ability of polar bears to migrate vast distances over the northern Arctic has been demonstrated using telemetry tracking; a single female moved from Kane Basin (west coast) northward around Greenland to Russia, a distance of ~2000 km (52). Our habitat models are based exclusively on coarse-scale abiotic factors and thus assume no demographic or local-scale geographic barriers. Therefore, the observed differentiation between west and east coast bears may well reflect biotic factors. Our stable isotope ecological proxy data support this and reveal ecological distinctions between bears sampled from each coast (Fig. 2). Different ocean currents result in a longer open-water season and higher productivity along the west Greenland coast and a much less productive marine environment along the east coast, where sea ice cover is more extensive in both time and space (Fig. 1A) (53). These differing ocean currents and levels of productivity could be the ecological driver, as variation at the base of food webs has bottom-up effects on ecosystem structure and function as a whole (13). In addition, our stable isotope analysis of five pinniped species (Fig. 2) revealed that differences between geographic localities reflect both discrepancies in the type of prey species consumed and in the underlying primary producers, i.e., relative abundance of sea ice microalgae and phytoplankton, as has been shown in narwhals, another Arctic marine predator (31).

The dietary plasticity of polar bears indicated by our findings may be a key attribute in the resilience of the species, acting to buffer the relatively low levels of genetic variation on which selection can act (21, 28, 54). Prey abundances are much lower in east Greenland, and, therefore, bears in this region may be especially prone to dietary shifts (55). Dietary shifts in east Greenland polar bears due to sea ice reduction in recent decades have been reported, with a decline in ringed seal consumption and an increase in harp seals and hooded seals (56, 57)—a finding supported by our data (Fig. 2). In addition, polar bear population density may also play an important role. However, we are limited in our ability to elucidate this further as census size estimates for the East Greenland management unit are unavailable (55).

The tendency for larger skull size, and by proxy larger body size/mass (58), in bears sampled in west Greenland (Fig. 3) may reflect underlying genetic mechanisms. We did detect two genes associated with body height [*SDCCAG8* (36) and *DNASE1L3* (37)] and one associated with body mass [*MAST3* (37)] to be in genomic regions highly differentiated between populations. Furthermore, we uncovered several highly differentiated regions in noncoding

regions of the genome, which, while their function is currently unknown, may play an important role in gene regulatory networks (59). An alternative hypothesis is that differences may be driven by phenotypic plasticity and adaptation to the unique diets on each coast; the ability of west Greenland bears to grow larger than their east Greenland counterparts may reflect the relatively higher amounts and/or more nutrient-rich food in the more productive west (53).

In east Greenland, size differences between sexes may have driven additional ecological divergence; higher $\delta^{13}\text{C}$ and $\delta^{15}\text{N}$ values in males (Fig. 2B) indicated the incorporation of larger amounts of bearded seals in their diets, while females consumed primarily ringed seals and harp seals. Larger males have a greater capacity to successfully hunt larger prey than smaller females, and bearded and hooded seals are larger (60). Therefore, because of a decline in the availability of smaller prey, east Greenland males may hunt larger prey. This is supported by their wider posterior skulls (Fig. 3A)—particularly around the temporal fossa, where the temporalis muscle that operates the mandible attaches, suggesting more muscular heads and adaptation to larger prey species. If ringed seals are the optimal polar bear prey species in terms of energetic return for energy input, the finding in west Greenland may be driven by higher productivity and greater prey availability, allowing both males and females to converge on the same diet (61).

Our study demonstrates the long-term association between demographic change and environmental perturbations in an Arctic top predator. The indirect connection of the polar bear to lower trophic levels can therefore be used to infer ecological dynamics across millennia. Collectively, our results suggest that the size and connectivity of polar bear populations around Greenland have been negatively influenced by past increases in SST, decreases in sea ice cover, and losses in the southern parts of the range, in line with predictions of contemporary populations (46). However, our findings also suggest that bears may ecologically adapt relatively rapidly. This ability is crucial for their resilience to ongoing rapid shifts in the distribution and abundance of prey caused by anthropogenic climate change (62). Adaptation through phenotypic and/or ecological shifts is more rapid than by DNA nucleotide changes and is a major factor allowing species to survive conditions of accelerating changes in climate and food availability (63). However, even with behavioral and phenotypic plasticity, the pace and scale of predicted near-future ecological change in the Arctic (51), coupled with a long generation time, are likely to leave polar bears vulnerable to climate and environmental change in the near future.

MATERIALS AND METHODS

This study focused on polar bear individuals sampled around Greenland, which were analyzed using a combination of genomics, stable isotopes, morphometrics, and ecological modeling. The polar bears were divided by geographic locality into the west and east coasts, the former representing the management units of Kane Basin and Baffin Bay and the latter representing the East Greenland management unit.

Using genome-wide resequencing data (raw paired-end Illumina fastq files) available from polar bear individuals sampled around Greenland (Kane Basin, $n = 27$; Baffin Bay, $n = 18$; East Greenland, $n = 37$) (21, 26, 28, 64), we performed genomic analyses to investigate (i) patterns of diversity and substructuring among bears

inhabiting the different coasts, (ii) each coast's respective demographic history, and (iii) the potential selective outcomes driven by the different environments of each coast. To understand the evolutionary relationships of the Greenland individuals within a wider geographic context, we also included available genomic data from polar bears of the adjoining subpopulations on either side of Greenland: Canada, $n = 3$ (64), and Svalbard, $n = 18$ (28). All data are available from the National Center for Biotechnology Information under the following Bioproject IDs: PRJNA169236, PRJNA196978, PRJNA210951, and PRJNA669153.

We used stable isotope analyses of bone collagen carbon ($\delta^{13}\text{C}$) and nitrogen ($\delta^{15}\text{N}$) to investigate the differences in prey choice between bears inhabiting the west and east coasts and between males and females on the same coast (Kane Basin, $n = 7$; Baffin Bay, $n = 6$; and East Greenland, $n = 18$) (table S4). To control for region-specific differences in primary productivity, we also performed bone collagen stable $\delta^{13}\text{C}$ and $\delta^{15}\text{N}$ isotope measurements of the five main putative pinniped prey species of polar bears (20, 65): bearded seals, harp seals, hooded seals, ringed seals, and walrus (*Odobenus rosmarus*). The total of 110 pinniped specimens analyzed represented 54 individuals from the west coast and 56 individuals from the east coast of Greenland (table S4).

We used geometric morphometric analyses to investigate any differences in skull size and shape between bears inhabiting the two coasts and between males and females within coasts. We analyzed a total of 134 specimens [Kane Basin, $n = 14$ (7♀, 7♂); Baffin Bay, $n = 14$ (7♀, 7♂); East Greenland, $n = 106$ (58♀, 48♂)] (table S5). The skulls were sampled between 1936 and 2015, and we make the assumption that skull size and shape did not change through this period.

There was partial overlap between the polar bear samples used for the genomic, stable isotope and geometric morphometric analyses (tables S1, S4, and S5). One sample overlapped in the genomic and stable isotope analyses, 6 samples overlapped between the genomic and geometric morphometric analyses, and 26 samples overlapped between the stable isotope and geometric morphometric analyses.

To understand Holocene climatic and environmental changes around Greenland and how they may have influenced the degree of suitable habitat for polar bears, we compiled polar bear occurrence records from the early 20th century to the end of 2019 and used ecological niche modeling (ENM) to estimate the area of suitable habitat over the past 11,000 years. Detailed information of all analyses is provided in the Supplementary Materials.

Supplementary Materials

This PDF file includes:

Supplementary Methods
Supplementary Text
Figs. S1 to S13
Legends for tables S1 to S6
Legend for movie S1
Legend for data S1
References

Other Supplementary Material for this manuscript includes the following:

Tables S1 to S6
Movie S1
Data S1

REFERENCES AND NOTES

- A. Dai, D. Luo, M. Song, J. Liu, Arctic amplification is caused by sea-ice loss under increasing CO₂. *Nat. Commun.* **10**, 121 (2019).
- M. Meredith, M. Sommerkorn, S. Cassotta, C. Derksen, A. Ekaykin, A. Hollowed, G. Kofinas, A. Mackintosh, J. Melbourne-Thomas, M. M. C. Muelbert, G. Ottersen, H. Pritchard, E. A. G. Schuur, Polar regions, in *IPCC Special Report on the Ocean and Cryosphere in a Changing Climate*, H.-O. Pörtner, D. C. Roberts, V. Masson-Delmotte, P. Zhai, M. Tignor, E. Poloczanska, K. Mintenbeck, A. Alegria, M. Nicolai, A. Okem, J. Petzold, B. Rama, N. M. Weyerin, Eds. (Cambridge University, 2019), chap. 3, pp. 203–320. https://repository.library.noaa.gov/view/noaa/27411/noaa_27411_DS1.pdf.
- C. M. Duarte, S. Agustí, P. Wassmann, J. M. Arrieta, M. Alcaraz, A. Coello, N. Marbà, I. E. Hendriks, J. Holding, I. García-Zarandona, E. Kritzberg, D. Vagué, Tipping elements in the Arctic marine ecosystem. *Ambio* **41**, 44–55 (2012).
- D. I. Armstrong McKay, A. Staal, J. F. Abrams, R. Winkelmann, B. Sakschewski, S. Loriani, I. Fetzer, S. E. Cornell, J. Rockström, T. M. Lenton, Exceeding 1.5°C global warming could trigger multiple climate tipping points. *Science* **377**, eabn7950 (2022).
- J. E. Box, W. T. Colgan, T. R. Christensen, N. M. Schmidt, M. Lund, F.-J. W. Parmentier, R. Brown, U. S. Bhatt, E. S. Euskirchen, V. E. Romanovsky, J. E. Walsh, J. E. Overland, M. Wang, R. W. Corell, W. N. Meier, B. Wouters, S. Mernild, J. Mård, J. Pawlak, M. S. Olsen, Key indicators of Arctic climate change: 1971–2017. *Environ. Res. Lett.* **14**, 045010 (2019).
- S. Ribeiro, A. Limoges, G. Massé, K. L. Johansen, W. Colgan, K. Weckström, R. Jackson, E. Georgiadis, N. Mikkelsen, A. Kuijpers, J. Olsen, S. M. Olsen, M. Nissen, T. J. Andersen, A. Strunk, S. Wetterich, J. Syvärianta, A. C. G. Henderson, H. Mackay, S. Taipale, E. Jeppesen, N. K. Larsen, X. Crosta, J. Giraudeau, S. Wengrat, M. Nuttall, B. Grønnow, A. Mosbech, T. A. Davidson, Vulnerability of the North Water ecosystem to climate change. *Nat. Commun.* **12**, 4475 (2021).
- D. A. Fordham, S. T. Jackson, S. C. Brown, B. Huntley, B. W. Brook, D. Dahl-Jensen, M. T. P. Gilbert, B. L. Otto-Bliesner, A. Svensson, S. Theodoridis, J. M. Wilmschurst, J. C. Buettel, E. Canteri, M. McDowell, L. Orlando, J. Pilowsky, C. Rahbek, D. Nogués-Bravo, Using paleo-archives to safeguard biodiversity under climate change. *Science* **369**, eabc5654 (2020).
- F. S. Amand, S. T. Childs, E. J. Reitz, S. Heller, B. Newsom, T. C. Rick, D. H. Sandweiss, R. Wheeler, Leveraging legacy archaeological collections as proxies for climate and environmental research. *Proc. Natl. Acad. Sci. U.S.A.* **117**, 8287–8294 (2020).
- M. J. Hopwood, D. Carroll, T. J. Browning, L. Meire, J. Mortensen, S. Krisch, E. P. Achterberg, Non-linear response of summertime marine productivity to increased meltwater discharge around Greenland. *Nat. Commun.* **9**, 3256 (2018).
- M. J. Hopwood, D. Carroll, T. Dunse, A. Hodson, J. M. Holding, J. L. Iriarte, S. Ribeiro, E. P. Achterberg, C. Cantoni, D. F. Carlson, Review article: How does glacier discharge affect marine biogeochemistry and primary production in the Arctic? *Cryosphere* **14**, 1347–1383 (2020).
- E. Buch, S. A. Pedersen, M. H. Ribergaard, Ecosystem variability in west Greenland waters. *J. Northw. Atl. Fish. Sci.* **34**, 13–28 (2004).
- K. R. Arrigo, D. K. Perovich, R. S. Pickart, Z. W. Brown, G. L. van Dijken, K. E. Lowry, M. M. Mills, M. A. Palmer, W. M. Balch, F. Bahr, N. R. Bates, C. Benitez-Nelson, B. Bowler, E. Brownlee, J. K. Ehn, K. E. Frey, R. Garley, S. R. Laney, L. Lubelczyk, J. Mathis, A. Matsuoka, B. G. Mitchell, G. W. K. Moore, E. Ortega-Retuerta, S. Pal, C. M. Polashenski, R. A. Reynolds, B. Schieber, H. M. Sosik, M. Stephens, J. H. Swift, Massive phytoplankton blooms under Arctic sea ice. *Science* **336**, 1408 (2012).
- M. Daase, J. Berge, J. E. Soreide, S. Falk-Petersen, Ecology of arctic pelagic communities, in *Arctic Ecology*, D. N. Thomas, Ed. (John Wiley & Sons Ltd., 2021), pp. 219–259.
- O. Gilg, K. M. Kovacs, J. Aars, J. Fort, G. Gauthier, D. Grémillet, R. A. Ims, H. Meltofte, J. Moreau, E. Post, N. M. Schmidt, G. Yannic, L. Bollache, Climate change and the ecology and evolution of Arctic vertebrates. *Ann. N. Y. Acad. Sci.* **1249**, 166–190 (2012).
- C. R. Harington, The evolution of Arctic marine mammals. *Ecol. Appl.* **18** (Suppl. 2), S23–S40 (2008).
- A. E. Rosenblatt, O. J. Schmitz, Climate change, nutrition, and bottom-up and top-down food web processes. *Trends Ecol. Evol.* **31**, 965–975 (2016).
- T. A. Brown, M. P. Galicia, G. W. Thiemann, S. T. Belt, D. J. Yurkowski, M. G. Dyck, High contributions of sea ice derived carbon in polar bear (*Ursus maritimus*) tissue. *PLOS One* **13**, e0191631 (2018).
- K. L. Laidre, I. Stirling, L. F. Lowry, Ø. Wiig, M. P. Heide-Jørgensen, S. H. Ferguson, Quantifying the sensitivity of Arctic marine mammals to climate-induced habitat change. *Ecol. Appl.* **18**, S97–S125 (2008).
- S. C. Amstrup, D. P. DeMaster, Polar bear, *Ursus maritimus*, in *Wild Mammals of North America: Biology, Management, and Conservation*, G. A. Feldhamer, B. C. Thompson, J. A. Chapman, Eds. (John Hopkins University Press, 2003), pp 587–610.
- I. Stirling, Polar Bear: *Ursus maritimus*, in *Encyclopedia of Marine Mammals (Second Edition)*, W. F. Perrin, B. Würsig, J. G. M. Thewissen, Eds. (Academic Press, 2009), pp. 888–890.
- S. Liu, E. D. Lorenzen, M. Fumagalli, B. Li, K. Harris, Z. Xiong, L. Zhou, T. S. Korneliusen, M. Somel, C. Babbitt, G. Wray, J. Li, W. He, Z. Wang, W. Fu, X. Xiang, C. C. Morgan, A. Doherty, M. J. O'Connell, J. O. McInerney, E. W. Born, L. Dalén, R. Dietz, L. Orlando, C. Sonne, G. Zhang, R. Nielsen, E. Willerslev, J. Wang, Population genomics reveal recent speciation and rapid evolutionary adaptation in polar bears. *Cell* **157**, 785–794 (2014).
- D. Paetkau, S. C. Amstrup, E. W. Born, W. Calvert, A. E. Derocher, G. W. Garner, F. Messier, I. Stirling, M. K. Taylor, O. Wiig, C. Strobeck, Genetic structure of the world's polar bear populations. *Mol. Ecol.* **8**, 1571–1584 (1999).
- G. M. Durner, K. L. Laidre, G. S. York, Polar bears, in *Proceedings of the 18th Working Meeting of the IUCN/SSC Polar Bear Specialist Group*, 7–11 June 2016, Anchorage, Alaska, Gland, Switzerland and Cambridge (UK: IUCN, 2018), xxx + pp. 207. <https://portals.iucn.org/library/efiles/documents/SSC-OP-063-En.pdf>.
- M. Mauritzen, A. E. Derocher, O. Wiig, S. E. Belikov, A. N. Boltunov, E. Hansen, G. W. Garner, Using satellite telemetry to define spatial population structure in polar bears in the Norwegian and western Russian Arctic. *J. Appl. Ecol.* **39**, 79–90 (2002).
- M. E. Obbard, G. W. Thiemann, E. Peacock, T. D. DeBruyn, Eds., Polar bears, in *Proceedings of the 15th Working Meeting of the IUCN/SSC Polar Bear Specialist Group*, Copenhagen, Denmark, 29 June to 3 July 2009 (IUCN, Gland, Switzerland and Cambridge, UK, 2010), vii + pp. 235.
- K. L. Laidre, M. A. Supple, E. W. Born, E. V. Regehr, Ø. Wiig, F. Ugarte, J. Aars, R. Dietz, C. Sonne, P. Hegelund, C. Isaksen, G. B. Akse, B. Cohen, H. L. Stern, T. Moon, C. Vollmers, R. Corbett-Detig, D. Paetkau, B. Shapiro, Glacial ice supports a distinct and undocumented polar bear subpopulation persisting in late 21st-century sea-ice conditions. *Science* **376**, 1333–1338 (2022).
- T. C. Rick, R. Lockwood, Integrating paleobiology, archeology, and history to inform biological conservation. *Conserv. Biol.* **27**, 45–54 (2013).
- W. Miller, S. C. Schuster, A. J. Welch, A. Ratan, O. C. Bedoya-Reina, F. Zhao, H. L. Kim, R. C. Burhans, D. I. Drautz, N. E. Wittekindt, L. P. Tomsho, E. Ibarra-Laclette, L. Herrera-Estrella, E. Peacock, S. Farley, G. K. Sage, K. Rode, M. Obbard, R. Montiel, L. Bachmann, O. Ingólfsson, J. Aars, T. Mailund, O. Wiig, S. L. Talbot, C. Lindqvist, Polar and brown bear genomes reveal ancient admixture and demographic footprints of past climate change. *Proc. Natl. Acad. Sci. U.S.A.* **109**, E2382–E2390 (2012).
- N. Boucher, A. E. Derocher, E. S. Richardson, Variability in polar bear *Ursus maritimus* stable isotopes in relation to environmental change in the Canadian Beaufort Sea. *Mar. Ecol. Prog. Ser.* **630**, 215–225 (2019).
- C. Kebaili, S. Sherpa, D. Rioux, L. Després, Demographic inferences and climatic niche modelling shed light on the evolutionary history of the emblematic cold-adapted Apollo butterfly at regional scale. *Mol. Ecol.* **31**, 448–466 (2022).
- M. Louis, M. Skovrind, E. Garde, M. P. Heide-Jørgensen, P. Szpak, E. D. Lorenzen, Population-specific sex and size variation in long-term foraging ecology of belugas and narwhals. *R. Soc. Open Sci.* **8**, 202226 (2021).
- M. Pigliucci, Evolution of phenotypic plasticity: Where are we going now? *Trends Ecol. Evol.* **20**, 481–486 (2005).
- H. Li, R. Durbin, Inference of human population history from individual whole-genome sequences. *Nature* **475**, 493–496 (2011).
- X. Liu, Y.-X. Fu, Exploring population size changes using SNP frequency spectra. *Nat. Genet.* **47**, 555–559 (2015).
- F. Tajima, Statistical method for testing the neutral mutation hypothesis by DNA polymorphism. *Genetics* **123**, 585–595 (1989).
- G. Kichaev, G. Bhatia, P.-R. Loh, S. Gazal, K. Burch, M. K. Freund, A. Schoech, B. Pasaniuc, A. L. Price, Leveraging polygenic functional enrichment to improve GWAS power. *Am. J. Hum. Genet.* **104**, 65–75 (2019).
- I. Tachmazidou, D. Süveges, J. L. Min, G. R. S. Ritchie, J. Steinberg, K. Walter, V. Lotchkova, J. Schwartzentruber, J. Huang, Y. Memari, S. McCarthy, A. A. Crawford, C. Bombieri, M. Cocca, A.-E. Farnaki, T. R. Gaunt, P. Jousilahti, M. N. Koopman, B. Lehne, G. Malerba, S. Männistö, A. Matchan, C. Medina-Gomez, J. F. Metrustry, A. Nag, I. Ntalla, L. Paternoster, N. W. Rayner, C. Sala, W. R. Scott, H. A. Shihab, L. Southam, B. S. Pourcain, M. Traglia, K. Trajanoska, G. Zaza, W. Zhang, M. S. Artigas, N. Bansal, M. Benn, Z. Chen, P. Danecek, W.-Y. Lin, A. Locke, J. Luan, A. K. Manning, A. Mulas, C. Sidore, A. Tybjaerg-Hansen, A. Varbo, M. Zoledziowska, C. Finan, K. Hatzikotoulas, A. E. Hendricks, J. P. Kemp, A. Moayyeri, K. Panoutsopoulou, M. Szpak, S. G. Wilson, M. Boehnke, F. Cucca, E. Di Angelantonio, C. Langenberg, C. Lindgren, M. I. McCarthy, A. P. Morris, B. G. Nordestgaard, R. A. Scott, M. D. Tobin, N. J. Wareham; SpiroMeta Consortium; GoT2D Consortium; P. Burton, J. C. Chambers, G. D. Smith, G. Dedoussis, J. F. Felix, O. H. Franco, G. Gambaro, P. Gasparini, C. J. Hammond, A. Hofman, V. W. V. Jaddoe, M. Kleber, J. S. Kooner, M. Perola, C. Relton, S. M. Ring, F. Rivadeneira, V. Salomaa, T. D. Spector, O. Stegle, D. Toniolo, A. G. Uitterlinden; arcOGEN Consortium, Understanding Society Scientific Group, UK10K Consortium, I. Barroso, C. M. T. Greenwood, J. R. B. Perry, B. R. Walker, A. S. Butterworth, Y. Xue, R. Durbin, K. S. Small, N. Soranzo, N. J. Timpson, E. Zeggini, Whole-genome sequencing

- coupled to imputation discovers genetic signals for anthropometric traits. *Am. J. Hum. Genet.* **100**, 865–884 (2017).
38. M. P. Galicia, G. W. Thiemann, M. G. Dyck, S. H. Ferguson, Characterization of polar bear (*Ursus maritimus*) diets in the Canadian High Arctic. *Polar Biol.* **38**, 1983–1992 (2015).
 39. C. Merow, M. J. Smith, J. A. Silander Jr., A practical guide to MaxEnt for modeling species' distributions: What it does, and why inputs and settings matter. *Ecography* **36**, 1058–1069 (2013).
 40. C. Buizert, B. A. Keisling, J. E. Box, F. He, A. E. Carlson, G. Sinclair, R. M. DeConto, Greenland-wide seasonal temperatures during the last deglaciation. *Geophys. Res. Lett.* **45**, 1905–1914 (2018).
 41. A. E. Jennings, J. T. Andrews, C. Ó. Cofaigh, G. S. Onge, C. Sheldon, S. T. Belt, P. Cabedo-Sanz, C. Hillaire-Marcel, Ocean forcing of Ice Sheet retreat in central west Greenland from LGM to the early Holocene. *Earth Planet. Sci. Lett.* **472**, 1–13 (2017).
 42. V. Sahanaïen, A. E. Derocher, Monitoring sea ice habitat fragmentation for polar bear conservation. *Anim. Conserv.* **15**, 397–406 (2012).
 43. K. D. Rode, E. Peacock, M. Taylor, I. Stirling, E. W. Born, K. L. Laidre, Ø. Wiig, A tale of two polar bear populations: Ice habitat, harvest, and body condition. *Popul. Ecol.* **54**, 3–18 (2012).
 44. K. L. Laidre, S. Atkinson, E. V. Regehr, H. L. Stern, E. W. Born, Ø. Wiig, N. J. Lunn, M. Dyck, Interrelated ecological impacts of climate change on an apex predator. *Ecol. Appl.* **30**, e02071 (2020).
 45. E. V. Regehr, N. J. Lunn, S. C. Amstrup, I. Stirling, Effects of earlier sea ice breakup on survival and population size of polar bears in western Hudson Bay. *J. Wildl. Manage.* **71**, 2673–2683 (2007).
 46. E. V. Regehr, K. L. Laidre, H. R. Akçakaya, S. C. Amstrup, T. C. Atwood, N. J. Lunn, M. Obbard, H. Stern, G. W. Thiemann, Ø. Wiig, Conservation status of polar bears (*Ursus maritimus*) in relation to projected sea-ice declines. *Biol. Lett.* **12**, 20160556 (2016).
 47. Y. Axford, A. de Vernal, E. C. Osterberg, Past warmth and its impacts during the holocene thermal maximum in greenland. *Annu. Rev. Earth Planet. Sci.* **49**, 279–307 (2021).
 48. E. Armstrong, P. O. Hopcroft, P. J. Valdes, Author correction: A simulated Northern Hemisphere terrestrial climate dataset for the past 60,000 years. *Sci Data* **7**, 91 (2020).
 49. D. A. Fordham, F. Saltré, S. C. Brown, C. Mellin, T. M. L. Wigley, Why decadal to century timescale palaeoclimate data are needed to explain present-day patterns of biological diversity and change. *Glob. Chang. Biol.* **24**, 1371–1381 (2018).
 50. J. M. Gutiérrez, R. G. Jones, G. T. Narisma, L. M. Alves, M. Amjad, I. V. Gorodetskaya, M. Grose, N. A. B. Klutse, S. Krakovska, J. Li, D. Martínez-Castro, L. O. Mearns, S. Atlas, in *Climate Change 2021: The Physical Science Basis. Contribution of Working Group I to the Sixth Assessment Report of the Intergovernmental Panel on Climate Change*, Masson-Delmotte, V., P. Zhai, A. Pirani, S. L. Connors, C. Péan, S. Berger, N. Caud, Y. Chen, L. Goldfarb, M. I. Gomis, M. Huang, K. Leitzell, E. Lonnoy, J. B. R. Matthews, T. K. Maycock, T. Waterfield, O. Yelekçi, R. Yu, B. Zhou, Eds. (Cambridge University Press, 2021), pp. 1927–2058.
 51. B. Fox-Kemper, H. T. Hewitt, C. Xiao, G. Aðalgeirsdóttir, S. S. Drijfhout, T. L. Edwards, N. R. Golledge, M. Hemer, R. E. Kopp, G. Krinner, A. Mix, D. Notz, S. Nowicki, I. S. Nurhati, L. Ruiz, J.-B. Sallée, A. B. A. Slangen, Y. Yu, Ocean, cryosphere and sea level change, in *Climate Change 2021: The Physical Science Basis. Contribution of Working Group I to the Sixth Assessment Report of the Intergovernmental Panel on Climate Change*, Masson-Delmotte, V., P. Zhai, A. Pirani, S. L. Connors, C. Péan, S. Berger, N. Caud, Y. Chen, L. Goldfarb, M. I. Gomis, M. Huang, K. Leitzell, E. Lonnoy, J. B. R. Matthews, T. K. Maycock, T. Waterfield, O. Yelekçi, R. Yu, B. Zhou, Eds. (Cambridge University Press, 2021), pp. 1211–1362.
 52. K. L. Laidre, S. N. Atkinson, E. V. Regehr, H. L. Stern, E. W. Born, Ø. Wiig, N. J. Lunn, M. Dyck, P. Heagerty, B. R. Cohen, Transient benefits of climate change for a high-Arctic polar bear (*Ursus maritimus*) subpopulation. *Glob. Chang. Biol.* **26**, 6251–6265 (2020).
 53. C. Michel, J. Hamilton, E. Hansen, D. Barber, M. Reigstad, J. Iacozza, L. Seuthe, A. Niemi, Arctic Ocean outflow shelves in the changing Arctic: A review and perspectives. *Prog. Oceanogr.* **139**, 66–88 (2015).
 54. J. A. S. Castruita, M. V. Westbury, E. D. Lorenzen, Analyses of key genes involved in Arctic adaptation in polar bears suggest selection on both standing variation and de novo mutations played an important role. *BMC Genomics* **21**, 543 (2020).
 55. K. L. Laidre, H. Stern, K. M. Kovacs, L. Lowry, S. E. Moore, E. V. Regehr, S. H. Ferguson, Ø. Wiig, P. Boveng, R. P. Angliss, E. W. Born, D. Litovka, L. Quakenbush, C. Lydersen, D. Vongraven, F. Ugarte, Arctic marine mammal population status, sea ice habitat loss, and conservation recommendations for the 21st century. *Conserv. Biol.* **29**, 724–737 (2015).
 56. M. A. McKinney, S. J. Iverson, A. T. Fisk, C. Sonne, F. F. Rigét, R. J. Letcher, M. T. Arts, E. W. Born, A. Rosing-Asvid, R. Dietz, Global change effects on the long-term feeding ecology and contaminant exposures of East Greenland polar bears. *Glob. Chang. Biol.* **19**, 2360–2372 (2013).
 57. R. Dietz, J.-P. Desforages, K. Gustavson, F. F. Rigét, E. W. Born, R. J. Letcher, C. Sonne, Immunologic, reproductive, and carcinogenic risk assessment from POP exposure in East Greenland polar bears (*Ursus maritimus*) during 1983–2013. *Environ. Int.* **118**, 169–178 (2018).
 58. A. E. Derocher, Ø. Wiig, Postnatal growth in body length and mass of polar bears (*Ursus maritimus*) at Svalbard. *J. Zool.* **256**, 343–349 (2002).
 59. G. A. Maston, S. K. Evans, M. R. Green, Transcriptional regulatory elements in the human genome. *Annu. Rev. Genomics Hum. Genet.* **7**, 29–59 (2006).
 60. A. E. Derocher, M. Andersen, Ø. Wiig, Sexual dimorphism of polar bears. *J. Mammal.* **86**, 895–901 (2005).
 61. D. I. Bolnick, P. Amarasekare, M. S. Araújo, R. Bürger, J. M. Levine, M. Novak, V. H. W. Rudolf, S. J. Schreiber, M. C. Urban, D. A. Vasseur, Why intraspecific trait variation matters in community ecology. *Trends Ecol. Evol.* **26**, 183–192 (2011).
 62. C. D. Hamilton, J. Vacquière-García, K. M. Kovacs, R. A. Ims, J. Kohler, C. Lydersen, Contrasting changes in space use induced by climate change in two Arctic marine mammal species. *Biol. Lett.* **15**, 20180834 (2019).
 63. Steppe brown bear *Ursus arctos* "priscus" from the Late Pleistocene of Europe. *Quat. Int.* **534**, 158–170 (2019).
 64. J. A. Cahill, R. E. Green, T. L. Fulton, M. Stiller, F. Jay, N. Ovsyanikov, R. Salamzade, J. St John, I. Stirling, M. Slatkin, B. Shapiro, Genomic evidence for island population conversion resolves conflicting theories of polar bear evolution. *PLOS Genet.* **9**, e1003345 (2013).
 65. I. Stirling, *Polar Bears* (University of Michigan Press, 1988).
 66. S. Bacon, A. Marshall, N. P. Holliday, Y. Aksenov, S. R. Dye, Seasonal variability of the East Greenland Coastal Current. *J. Geophys. Res. C: Oceans* **119**, 3967–3987 (2014).
 67. S. Rysgaard, W. Boone, D. Carlson, M. K. Sejr, J. Bendtsen, T. Juul-Pedersen, H. Lund, L. Meire, J. Mortensen, An updated view on water masses on the pan-west Greenland continental shelf and their link to proglacial fjords. *J. Geophys. Res. C: Oceans* **125**, e2019JC015564 (2020).
 68. M. Schubert, L. Ermini, C. Der Sarkissian, H. Jónsson, A. Ginolhac, R. Schaefer, M. D. Martin, R. Fernández, M. Kircher, M. McCue, E. Willerslev, L. Orlando, Characterization of ancient and modern genomes by SNP detection and phylogenomic and metagenomic analysis using PALEOMIX. *Nat. Protoc.* **9**, 1056–1082 (2014).
 69. M. Schubert, S. Lindgreen, L. Orlando, AdapterRemoval v2: rapid adapter trimming, identification, and read merging. *BMC Res. Notes* **9**, 88 (2016).
 70. H. Li, R. Durbin, Fast and accurate short read alignment with Burrows–Wheeler transform. *Bioinformatics* **25**, 1754–1760 (2009).
 71. H. Li, B. Handsaker, A. Wysoker, T. Fennell, J. Ruan, N. Homer, G. Marth, G. Abecasis, R. Durbin, 1000 Genome Project Data Processing Subgroup, The Sequence Alignment/Map format and SAMtools. *Bioinformatics* **25**, 2078–2079 (2009).
 72. Broad Institute, "Picard Toolkit" (2019); <http://broadinstitute.github.io/picard>.
 73. A. McKenna, M. Hanna, E. Banks, A. Sivachenko, K. Cibulskis, A. Kernytzky, K. Garimella, D. Altshuler, S. Gabriel, M. Daly, M. A. DePristo, The Genome Analysis Toolkit: A MapReduce framework for analyzing next-generation DNA sequencing data. *Genome Res.* **20**, 1297–1303 (2010).
 74. T. S. Korneliussen, A. Albrechtsen, R. Nielsen, ANGSD: Analysis of next generation sequencing data. *BMC Bioinformatics* **15**, 356 (2014).
 75. J. Meisner, A. Albrechtsen, Inferring population structure and admixture proportions in low-depth NGS data. *Genetics* **210**, 719–731 (2018).
 76. V. Link, A. Kousathanas, K. Veeramah, C. Sell, A. Scheu, D. Wegmann, ATLAS: Analysis tools for low-depth and ancient samples. *bioRxiv* 105346 (2017). <https://doi.org/10.1101/105346>.
 77. A. Kousathanas, C. Leuenberger, V. Link, C. Sell, J. Burger, D. Wegmann, Inferring heterozygosity from ancient and low coverage genomes. *Genetics* **205**, 317–332 (2017).
 78. R Core Team, "R: A language and environment for statistical computing" (2013); <http://uvigo.es/CRAN/web/packages/dplr/vignettes/intro-dplr.pdf>.
 79. K. Hanghøj, I. Moltke, P. A. Andersen, A. Manica, T. S. Korneliussen, Fast and accurate relatedness estimation from high-throughput sequencing data in the presence of inbreeding. *Gigascience* **8**, giz034 (2019).
 80. M. S. Rasmussen, G. Garcia-Erill, T. S. Korneliussen, C. Wiuf, A. Albrechtsen, Estimation of site frequency spectra from low-coverage sequencing data using stochastic EM reduces overfitting, runtime, and memory usage. *Genetics* **222**, iyac148 (2022).
 81. N. F. Saremi, J. Oppenheimer, C. Vollmers, B. O'Connell, S. A. Milne, A. Byrne, L. Yu, O. A. Ryder, R. E. Green, B. Shapiro, An annotated draft genome for the Andean bear, *Tremarctos ornatus*. *J. Hered.* **112**, 377–384 (2021).
 82. R. Li, W. Fan, G. Tian, H. Zhu, L. He, J. Cai, Q. Huang, Q. Cai, B. Li, Y. Bai, Z. Zhang, Y. Zhang, W. Wang, J. Li, F. Wei, H. Li, M. Jian, J. Li, Z. Zhang, R. Nielsen, D. Li, W. Gu, Z. Yang, Z. Xuan, O. A. Ryder, F. C.-C. Leung, Y. Zhou, J. Cao, X. Sun, Y. Fu, X. Fang, X. Guo, B. Wang, R. Hou, F. Shen, B. Mu, P. Ni, R. Lin, W. Qian, G. Wang, C. Yu, W. Nie, J. Wang, Z. Wu, H. Liang, J. Min, Q. Wu, S. Cheng, J. Ruan, M. Wang, Z. Shi, M. Wen, B. Liu, X. Ren, H. Zheng, D. Dong, K. Cook, G. Shan, H. Zhang, C. Kosiol, X. Xie, Z. Lu, H. Zheng, Y. Li, C. C. Steiner, T. T.-Y. Lam, S. Lin, Q. Zhang, G. Li, J. Tian, T. Gong, H. Liu, D. Zhang, L. Fang, C. Ye, J. Zhang, W. Hu, A. Xu,

- Y. Ren, G. Zhang, M. W. Bruford, Q. Li, L. Ma, Y. Guo, N. An, Y. Hu, Y. Zheng, Y. Shi, Z. Li, Q. Liu, Y. Chen, J. Zhao, N. Qu, S. Zhao, F. Tian, X. Wang, H. Wang, L. Xu, X. Liu, T. Vinar, Y. Wang, T.-W. Lam, S.-M. Yiu, S. Liu, H. Zhang, D. Li, Y. Huang, X. Wang, G. Yang, Z. Jiang, J. Wang, N. Qin, L. Li, J. Li, L. Bolund, K. Kristiansen, G. K.-S. Wong, M. Olson, X. Zhang, S. Li, H. Yang, J. Wang, J. Wang, The sequence and de novo assembly of the giant panda genome. *Nature* **463**, 311–317 (2010).
83. T. S. Korneliusson, I. Moltke, A. Albrechtsen, R. Nielsen, Calculation of Tajima's D and other neutrality test statistics from low depth next-generation sequencing data. *BMC Bioinformatics* **14**, 289 (2013).
84. H. Li, Protein-to-genome alignment with miniprot. *Bioinformatics* **39**, btad014 (2023).
85. K. Luu, E. Bazin, M. G. B. Blum, pcadapt: An R package to perform genome scans for selection based on principal component analysis. *Mol. Ecol. Resour.* **17**, 67–77 (2017).
86. L. Ricciardelli, S. D. Newsome, N. A. Dellabianca, R. Bastida, M. L. Fogel, R. N. P. Goodall, Ontogenetic diet shift in Commerson's dolphin (*Cephalorhynchus commersonii commersonii*) off Tierra del Fuego. *Polar Biol.* **36**, 617–627 (2013).
87. M. L. Fogel, N. Tuross, D. W. Owsley, Nitrogen isotope tracers of human lactation in modern and archaeological populations, in *Annual Report of the Director of the Geophysical Laboratory* (Carnegie Institution, 1989), vol. 88: pp. 111–117.
88. A. L. Bond, K. A. Hobson, B. A. Branfiren, Rapidly increasing methyl mercury in endangered ivory gull (*Pagophila eburnea*) feathers over a 130 year record. *Proc. Biol. Sci.* **282**, 20150032 (2015).
89. R. E. M. Hedges, J. G. Clement, C. D. L. Thomas, T. C. O'Connell, Collagen turnover in the adult femoral mid-shaft: Modeled from anthropogenic radiocarbon tracer measurements. *Am. J. Phys. Anthropol.* **133**, 808–816 (2007).
90. J. Folch, M. Lees, G. H. Sloane Stanley, A simple method for the isolation and purification of total LIPIDES from animal tissues. *J. Biol. Chem.* **226**, 497–509 (1957).
91. E. G. Bligh, W. J. Dyer, A rapid method of total lipid extraction and purification. *Can. J. Biochem. Physiol.* **37**, 911–917 (1959).
92. H. Qi, T. B. Coplen, H. Geilmann, W. A. Brand, J. K. Böhlke, Two new organic reference materials for $\delta^{13}\text{C}$ and $\delta^{15}\text{N}$ measurements and a new value for the $\delta^{13}\text{C}$ of NBS 22 oil. *Rapid Commun. Mass Spectrom.* **17**, 2483–2487 (2003).
93. H. Qi, T. B. Coplen, S. J. Mroczkowski, W. A. Brand, L. Brandes, H. Geilmann, A. Schimmelmann, A new organic reference material, L-glutamic acid, USGS41a, for $\delta^{13}\text{C}$ and $\delta^{15}\text{N}$ measurements – A replacement for USGS41. *Rapid Commun. Mass Spectrom.* **30**, 859–866 (2016).
94. P. Szpak, J. Z. Metcalfe, R. A. Macdonald, Best practices for calibrating and reporting stable isotope measurements in archaeology. *J. Archaeol. Sci. Rep.* **13**, 609–616 (2017).
95. C. D. Keeling, W. G. Mook, P. P. Tans, Recent trends in the $^{13}\text{C}/^{12}\text{C}$ ratio of atmospheric carbon dioxide. *Nature* **277**, 121–123 (1979).
96. M. Eide, A. Olsen, U. S. Ninnemann, T. Eldevik, A global estimate of the full oceanic ^{13}C Suess effect since the preindustrial: Full oceanic ^{13}C Suess effect. *Global Biogeochem. Cycles* **31**, 492–514 (2017).
97. G. M. Hilton, D. R. Thompson, P. M. Sagar, R. J. Cuthbert, Y. Cheres, S. J. Bury, A stable isotopic investigation into the causes of decline in a sub-Antarctic predator, the rock-hopper penguin *Eudyptes chrysocome*. *Eudyptes chrysocome*. *Glob. Chang. Biol.* **12**, 611–625 (2006).
98. N. Gruber, C. D. Keeling, R. B. Bacastow, P. R. Guenther, T. J. Lueker, M. Wahlen, H. A. J. Meijer, W. G. Mook, T. F. Stocker, Spatiotemporal patterns of carbon-13 in the global surface oceans and the oceanic Suess effect. *Global Biogeochem. Cycles* **13**, 307–335 (1999).
99. S. A. Mellon, "Investigating the ^{13}C Suess effect in the northwestern North Atlantic," thesis, Dalhousie University (2018).
100. K. L. Laidre, E. W. Born, S. N. Atkinson, Ø. Wiig, L. W. Andersen, N. J. Lunn, M. Dyck, E. V. Regehr, R. McGovern, P. Heagerty, Range contraction and increasing isolation of a polar bear subpopulation in an era of sea-ice loss. *Ecol. Evol.* **8**, 2062–2075 (2018).
101. R. Dietz, M.-P. Heide-Jørgensen, T. Härkönen, J. Teilmann, N. Valentin, Age determination of european harbour seal, *Phoca vitulina* L. *Sarsia* **76**, 17–21 (1991).
102. A. Rosing-Asvid, E. Born, M. Kingsley, Age at sexual maturity of males and timing of the mating season of polar bears (*Ursus maritimus*) in Greenland. *Polar Biol.* **25**, 878–883 (2002).
103. C. P. Klingenberg, MorphoJ: An integrated software package for geometric morphometrics. *Mol. Ecol. Resour.* **11**, 353–357 (2011).
104. C. P. Klingenberg, M. Barluenga, A. Meyer, Shape analysis of symmetric structures: Quantifying variation among individuals and asymmetry. *Evolution* **56**, 1909–1920 (2002).
105. Ø. Wiig, P. Henriksen, T. Sjøvold, E. W. Born, K. L. Laidre, R. Dietz, C. Sonne, J. Aars, Variation in non-metrical skull traits of polar bears (*Ursus maritimus*) and relationships across East Greenland and adjacent subpopulations (1830–2013). *Polar Biol.* **42**, 461–474 (2019).
106. P. A. Lachenbruch, An almost unbiased method of obtaining confidence intervals for the probability of misclassification in discriminant analysis. *Biometrics* **23**, 639–645 (1967).
107. G. M. Durner, D. C. Douglas, R. M. Nielson, S. C. Amstrup, T. L. McDonald, I. Stirling, M. Mauritzen, E. W. Born, Ø. Wiig, E. DeWeaver, M. C. Serreze, S. E. Belikov, M. M. Holland, J. Maslanik, J. Aars, D. A. Bailey, A. E. Derocher, Predicting 21st-century polar bear habitat distribution from global climate models. *Ecol. Monogr.* **79**, 25–58 (2009).
108. M. E. Aiello-Lammens, R. A. Boria, A. Radosavljevic, B. Vilela, R. P. Anderson, spThin: An R package for spatial thinning of species occurrence records for use in ecological niche models. *Ecography* **38**, 541–545 (2015).
109. M. B. Andrews, J. K. Ridley, R. A. Wood, T. Andrews, E. W. Blockley, B. Booth, E. Burke, A. J. Dittus, P. Florek, L. J. Gray, S. Haddad, S. C. Hardiman, L. Hermanson, D. Hodson, E. Hogan, G. S. Jones, J. R. Knight, T. Kuhlbrodt, S. Misios, M. S. Mizielski, M. A. Ringer, J. Robson, R. T. Sutton, Historical simulations with HadGEM3-GC3.1 for CMIP6. *J. Adv. Model. Earth Syst.* **12**, (2020).
110. V. Eyring, S. Bony, G. A. Meehl, C. A. Senior, B. Stevens, R. J. Stouffer, K. E. Taylor, Overview of the coupled model intercomparison project phase 6 (CMIP6) experimental design and organization. *Geosci. Model Dev.* **9**, 1937–1958 (2016).
111. P. J. Valdes, E. Armstrong, M. P. S. Badger, C. D. Bradshaw, F. Bragg, M. Crucifix, T. Davies-Barnard, J. J. Day, A. Farnsworth, C. Gordon, P. O. Hopcroft, A. T. Kennedy, N. S. Lord, D. J. Lunt, A. Marzocchi, L. M. Parry, V. Pope, W. H. G. Roberts, E. J. Stone, G. J. L. Tourte, J. H. T. Williams, The BRIDGE HadCM3 family of climate models: HadCM3@Bristol v1.0. *Geosci. Model Dev.* **10**, 3715–3743 (2017).
112. W. Dansgaard, S. J. Johnsen, H. B. Clausen, D. Dahl-Jensen, N. S. Gundestrup, C. U. Hammer, C. S. Hvidberg, J. P. Steffensen, A. E. Sveinbjörnsdóttir, J. Jouzel, G. Bond, Evidence for general instability of past climate from a 250-ka ice-core record. *Nature* **364**, 218–220 (1993).
113. H. Heinrich, Origin and consequences of cyclic ice rafting in the northeast Atlantic ocean during the past 130,000 years. *Quatern. Res.* **29**, 142–152 (1988).
114. T. P. Boyer, H. E. García, R. A. Locarnini, M. M. Zweng, A. V. Mishonov, J. R. Reagan, K. A. Weathers, O. K. Baeranova, C. R. Paver, D. Seidov, I. V. Smolyar, *World Ocean Atlas 2018* (NOAA National Centers for Environmental Information, 2021); <https://ncei.noaa.gov/archive/accession/NCEI-WOA18>.
115. G. P. Compo, J. S. Whitaker, P. D. Sardeshmukh, N. Matsui, R. J. Allan, X. Yin, B. E. Gleason, R. S. Vose, G. Rutledge, P. Bessemoulin, S. Brönnimann, M. Brunet, R. I. Crouthamel, A. N. Grant, P. Y. Groisman, P. D. Jones, M. C. Kruk, A. C. Kruger, G. J. Marshall, M. Mauger, H. Y. Mok, Ø. Nordli, T. F. Ross, R. M. Trigo, X. L. Wang, S. D. Woodruff, S. J. Worley, The twentieth century reanalysis project. *Q. J. R. Meteorol. Soc.* **137**, 1–28 (2011).
116. M. S. O'Donnell, D. A. Ignizio, Bioclimatic predictors for supporting ecological applications in the conterminous United States. *US geological survey data series* **691**, 4–9 (2012).
117. M. B. Araújo, R. P. Anderson, A. Márcia Barbosa, C. M. Beale, C. F. Dormann, R. Early, R. A. Garcia, A. Guisan, L. Maiorano, B. Naimi, R. B. O'Hara, N. E. Zimmermann, C. Rahbek, Standards for distribution models in biodiversity assessments. *Sci Adv* **5**, eaat4858 (2019).
118. M. P. Austin, Spatial prediction of species distribution: An interface between ecological theory and statistical modelling. *Ecol. Model.* **157**, 101–118 (2002).
119. J. Elith, J. R. Leathwick, Species distribution models: Ecological explanation and prediction across space and time. *Annu. Rev. Ecol. Syst.* **40**, 677–697 (2009).
120. N. P. Boucher, A. E. Derocher, E. S. Richardson, Spatial and temporal variability in ringed seal (*Pusa hispida*) stable isotopes in the Beaufort Sea. *Ecol. Evol.* **10**, 4178–4192 (2020).
121. K. Lone, K. M. Kovacs, C. Lydersen, M. Fedak, M. Andersen, P. Lovell, J. Aars, Aquatic behaviour of polar bears (*Ursus maritimus*) in an increasingly ice-free Arctic. *Sci. Rep.* **8**, 9677 (2018).
122. S. Joly, S. Senneville, D. Caya, F. J. Saucier, Sensitivity of Hudson Bay Sea ice and ocean climate to atmospheric temperature forcing. *Climate Dynam.* **36**, 1835–1849 (2011).
123. B. A. Bluhm, R. Gradinger, Regional variability in food availability for Arctic marine mammals. *Ecol. Appl.* **18** (Suppl 2), S77–S96 (2008).
124. S. Phillips, "maxnet: Fitting "Maxent" species distribution models with "glmnet" R package version 0.1.2" (2017); <https://CRAN.R-project.org/package=maxnet>.
125. S. J. Phillips, R. P. Anderson, R. E. Schapire, Maximum entropy modeling of species geographic distributions. *Ecol. Model.* **190**, 231–259 (2006).
126. R. Valavi, G. Guillera-Aroita, J. J. Lahoz-Monfort, J. Elith, Predictive performance of presence-only species distribution models: A benchmark study with reproducible code. *Ecol. Monogr.* **92**, e01486 (2022).
127. J. M. Kass, R. Muscarella, P. J. Galante, C. L. Bohl, G. E. Pinilla-Buitrago, R. A. Boria, M. Soley-Guardia, R. P. Anderson, ENMeval 2.0: Redesigned for customizable and reproducible modeling of species' niches and distributions. *Methods Ecol. Evol.* **12**, 1602–1608 (2021).
128. R. Valavi, J. Elith, J. J. Lahoz-Monfort, G. Guillera-Aroita, blockCV: Anrpackage for generating spatially or environmentally separated folds fork-fold cross-validation of species distribution models. *Methods Ecol. Evol.* **10**, 225–232 (2019).

129. S. C. Amstrup, B. G. Marcot, D. C. Douglas, A Bayesian network modeling approach to forecasting the 21st century worldwide status of polar bears, in *Arctic Sea Ice Decline: Observations, Projections, Mechanisms, and Implications* (American Geophysical Union, Washington, DC, 2008), vol. 180, pp. 213–268.
130. J. Elith, S. J. Phillips, T. Hastie, M. Dudik, Y. E. Chee, C. J. Yates, A statistical explanation of MaxEnt for ecologists. *Divers. Distrib.* **17**, 43–57 (2011).
131. C. F. Dormann, J. Elith, S. Bacher, C. Buchmann, G. Carl, G. Carré, J. R. G. Marquéz, B. Gruber, B. Lafourcade, P. J. Leitão, T. Münkemüller, C. McClean, P. E. Osborne, B. Reineking, B. Schröder, A. K. Skidmore, D. Zurell, S. Lautenbach, Collinearity: A review of methods to deal with it and a simulation study evaluating their performance. *Ecography* **36**, 27–46 (2013).
132. X. Feng, D. S. Park, Y. Liang, R. Pandey, M. Papeş, Collinearity in ecological niche modeling: Confusions and challenges. *Ecol. Evol.* **9**, 10365–10376 (2019).
133. B. W. Low, Y. Zeng, H. H. Tan, D. C. J. Yeo, Predictor complexity and feature selection affect Maxent model transferability: Evidence from global freshwater invasive species. *Divers. Distrib.* **27**, 497–511 (2021).
134. A. Radosavljević, R. Anderson, Making better Maxent models of species distributions: Complexity, overfitting and evaluation. *J. Biogeogr.* **41**, 629–643 (2014).
135. D. Nogués-Bravo, Predicting the past distribution of species climatic niches. *Glob. Ecol. Biogeogr.* **18**, 521–531 (2009).
136. Ocean Biodiversity Information System (OBIS), Intergovernmental Oceanographic Commission of UNESCO (2023); www.obis.org.
137. J. Mäkinen, J. Vanhatalo, Hierarchical Bayesian model reveals the distributional shifts of Arctic marine mammals. *Divers. Distrib.* **24**, 1381–1394 (2018).
138. E. Peacock, S. A. Sonsthagen, M. E. Obbard, A. Boltunov, E. V. Regehr, N. Ovsyanikov, J. Aars, S. N. Atkinson, G. K. Sage, A. G. Hope, E. Zeyl, L. Bachmann, D. Ehrlich, K. T. Scribner, S. C. Amstrup, S. Belikov, E. W. Born, A. E. Derocher, I. Stirling, M. K. Taylor, Ø. Wiig, D. Paetkau, S. L. Talbot, Implications of the circumpolar genetic structure of polar bears for their conservation in a rapidly warming Arctic. *PLOS One* **10**, e112021 (2015).
139. GBIF.org, GBIF Occurrence Download (11 March 2021); <https://doi.org/10.15468/dl.5hhypa>.
140. GBIF.org, GBIF Occurrence Download (27 May 2021); <https://doi.org/10.15468/dl.9ev52f>.
141. K. M. Kovacs, M. Andersen, *Marine Mammals Sightings in and around Svalbard 1995-2016* (Norwegian Polar Institute, 2010); <https://doi.org/10.21334/npolar.2010.246c1053>.
142. C. Lydersen, K. M. Kovacs, J. Aars, C. Hamilton, R. Ims, *Tracking data from polar bears (N=67, 2002–2004 & 2010–2013) and ringed seals (N=60, 2002–2004 & 2010–2012)* (Norwegian Polar Institute, 2017); <https://doi.org/10.21334/npolar.2017.132248b4>.
143. K. D. Rode, R. R. Wilson, E. V. Regehr, M. St. Martin, D. C. Douglas, J. Olson, *Data from: Increased Land Use by Chukchi Sea Polar Bears in Relation to Changing Sea Ice Conditions* (Dryad, 2016); <https://doi.org/10.5061/dryad.n5509>.
144. K. D. Rode, *Carbon and Nitrogen Isotope Concentrations in Polar Bear Hair and Prey from the Alaska Beaufort and Chukchi Seas, 1978-2019* (U.S. Geological Survey, 2021); <https://doi.org/10.5066/P9K5FT2>.
145. BOEM, Alaska Outer Continental Shelf (OCS) Region, N. M. F. S. NOAA, North Slope Borough, *Aerial Surveys of Arctic Marine Mammals (ASAMM) collected by Marine Mammal Laboratory, Bureau of Ocean Energy Management, and Other Agencies in the Bering, Chukchi, Beaufort Seas, and Amundsen Gulf from 1979 to 2019 and North Slope Borough, Alaska from 2020 to 2021* (NCEI Accession 0039614, National Centers for Environmental Information, 2008); <https://doi.org/10.7289/V51V5BZM>.
146. A. M. Pagano, T. C. Atwood, G. M. Durner, *Tracking Data Releases* (U.S. Geological Survey, 2019); <https://usgs.gov/centers/alaska-science-center/science/tracking-data-releases>.

Acknowledgments: We would like to acknowledge the large number of local hunters as well as J. Lorentzen and the late J. Brønlund who conducted the polar bear tissue sampling and organized the collection and shipment of samples in east Greenland. We thank L. Johannessen for assistance with seal samples from the National History Museum, University of Oslo (loan number DMA-30). Last, we would like to thank D. K. Johansson for assisting in locating the pinniped skulls at the Natural History Museum of Denmark. **Funding:** The work was supported by the Villum Fonden Young Investigator Programme grant no. 37352 to E.D.L., Independent Research Fund Denmark grant nos. 8021-002188 and 9064-00025B to E.D.L., the Carlsberg Foundation Distinguished Associate Professor Fellowship grant no. CF16-0202 to E.D.L., and an NSERC Discovery grant no. 2020-04740 to P.S. Polar bear skull samples collected over the past four decades by Aarhus University personnel were funded by the Danish Cooperation for Environment in the Arctic (DANCEA) (J.nr. 112-00144). A.A.C. was supported by a fellowship from Rubicon- NWO (project 019.183EN.005). **Author contributions:** Conceptualization: M.V.W. and E.D.L. Formal analysis: M.V.W., S.C.B., S.O., M.B.S., J.A.S.C., A.G., and P.S. Investigation: M.V.W., J.L., M.B.S., J.M., S.K.B., M.L., and A.A.C. Writing—original draft: M.V.W., S.R., A.G., and E.D.L. Writing—review and editing: All authors. Funding acquisition: E.D.L. Resources: E.A., R.D., C.S., P. S., and E.D.L. Supervision: D.A.F., P.S., and E.D.L. **Competing interests:** The authors declare that they have no competing interests. **Data and materials availability:** All data needed to evaluate the conclusions in the paper are present in the paper and/or the Supplementary Materials. Morphometric geometric coordinates are available as data S1. Example code for the genomic and stable isotope analyses can be found at <https://doi.org/10.5281/zenodo.8355187>. The data and scripts needed to replicate the habitat modeling can be found at <https://doi.org/10.5281/zenodo.8349059>.

Submitted 14 October 2022
Resubmitted 09 June 2023
Accepted 6 October 2023
Published 8 November 2023
10.1126/sciadv.adf3326

Impact of Holocene environmental change on the evolutionary ecology of an Arctic top predator

Michael V. Westbury, Stuart C. Brown, Julie Lorenzen, Stuart O'Neill, Michael B. Scott, Julia McCuaig, Christina Cheung, Edward Armstrong, Paul J. Valdes, José Alfredo Samaniego Castruita, Andrea A. Cabrera, Stine Keibel Blom, Rune Dietz, Christian Sonne, Marie Louis, Anders Galatius, Damien A. Fordham, Sofia Ribeiro, Paul Szpak, and Eline D. Lorenzen

Sci. Adv. **9** (45), eadf3326. DOI: 10.1126/sciadv.adf3326

View the article online

<https://www.science.org/doi/10.1126/sciadv.adf3326>

Permissions

<https://www.science.org/help/reprints-and-permissions>

Use of this article is subject to the [Terms of service](#)

Science Advances (ISSN 2375-2548) is published by the American Association for the Advancement of Science. 1200 New York Avenue NW, Washington, DC 20005. The title *Science Advances* is a registered trademark of AAAS.

Copyright © 2023 The Authors, some rights reserved; exclusive licensee American Association for the Advancement of Science. No claim to original U.S. Government Works. Distributed under a Creative Commons Attribution NonCommercial License 4.0 (CC BY-NC).